Interactions between demagnetizing field and minor-loop development in bulk ferromagnets ⋆

M. Kružík [a,*], T. Roubíček [b,a]

[a] *ÚTIA, Academy of Sciences, Pod vodárenskou věží 4, CZ-182 08 Praha 8, Czech Republic.*

[b] *Faculty of Mathematics and Physics, Charles University, Sokolovská 83, CZ-186 75 Praha 8, Czech Republic*

Abstract

A phenomenon of mutual influence of the demagnetizing field and a gradual increase of width of minor loops in bulk ferromagnets during magnetization processes is scrutinized by computational modeling. Classical static micromagnetics is here enriched by a suitable activated dissipation mechanism allowing for rate-independent hysteresis. The activation threshold is allowed to depend, again by a rate-independent manner, on local history of a magnetization process, which reflects (only on a mesoscopical level) gradual development of a domain structure. Influence of the shape of the specimen is thus automatically involved via nonlocal interactions through the demagnetizing field.

Key words: micromagnetism, maximal dissipation, hysteresis, vigin curve, computational simulations
PACS: 75.40Mg

⋆ Fruitful discussions with dr. Alfred Ludwig (caesar-Stiftung, Bonn) and dr. Ivan Tomáš (Institute of Physics, Prague) are acknowledged. This work was partly supported by the grants 201/00/0768 (GA ČR), A 107 5005 (GA AV ČR), and MSM 11320007 (MŠMT ČR). Both authors acknowledge the support of caesar-Stiftung during their stays at this institution in Bonn.

* Corresponding author: Institute of Information Theory and Automation, Academy of Sciences, Pod vodárenskou věží 4, CZ-182 08 Praha 8, Czech Republic. e-mail: kruzik@utia.cas.cz, fax: 00420-286-581-419, phone: 00420-266-052-395.

1 Introduction

The aim of this contribution is to study the mutual influence of the stray (demagnetizing) field and the gradual development of width of minor hysteresis loops (related with *activation threshold* for changing magnetization) during a magnetization process starting from a completely demagnetized specimen. Thus, indirectly, the shape of a ferromagnetic specimen is involved through long-distance interactions via this demagnetizing field. Microscopically, this minor-loop development is due to gradual evolution of the magnetic-domain structure during the magnetization process and, being analogous to gradual development of a dislocation structure in plastic materials during loading, is occasionally called hardening; we refer e.g. to Aktaa and von der Weth [2].

In this way, using only a few material data (which is, however, rather simplistic phenomenological description of complicated microscopical processes in domain structure evolution) together with information about the specimen shape, we can rigorously (at least as far the influence of a specimen shape on the resulting response) describe quite complex behavior of the specimen before the domain structure is fully developed in the whole bulk, i.e. complex hysteretic response inside the parent loop. In particular, it concerns the *virgin magnetization curve* describing a magnetization process of the demagnetized specimen to its magnetic saturation and various *minor loops* resulting from spatial inhomogeneities of the activation thresholds. The local phenomena, of course, interact non-locally with the whole bulk ferromagnet via the stray (demagnetizing) field whose energy favors a divergence free magnetization (in particular, its zero flux through the specimen boundary). Hence the virgin curve and the minor loops are related not only to a particular material but equally to the shape of the magnetized specimen. Although this phenomenon is qualitatively well-known in literature the rational quantitative study of it does not seem scrutinized so far.

The method, we use, is based on rigorous mathematical modeling especially as far as the nonlocal interactions concerns, combined with a certain phenomenology describing local properties of the material as well as with trustworthy physical principles of *minimization of Gibb's magnetic energy* competing with the *maximum-dissipation principle* governing rate-independent dissipative processes which are typical for hysteretic behavior of ferromagnets. The magnetic-domain microstructure is described by *volume fractions* expressed through Young's [40] parameterized probability measures, which we call a mesoscopical-level description [36,37], which advantageously compromises a microscopical full-detail pointwise description and macroscopical averaged description. We confine ourselves to *low-frequency* exterior magnetic fields which allows us to neglect all rate-dependent dissipation mechanisms and to simplify the full Maxwell system to the static situation, and we also confine ourselves

to considering only an *isothermal* case, assuming processes so slow that all heat produced by dissipation mechanisms can be transferred out.

Let us also mention that the activated dissipation is very natural in the context of ferromagnetism, and has been already used in a Jiles-Atherton-like model by Bergqvist [3], in a micromagnetic-type model and in a model based on macroscopical magnetization M (cf. (3)) by Visintin in [42] and [43], respectively. The mesoscopical description of the magnetization has been used by DeSimone [8], James and Kinderlehrer [13], and Rogers [33] (see also [17]) but in a mere Gibbs-energy minimization framework only.

2 The mesoscopical-level model

We briefly introduce a mathematical model which can capture the shape influence as outlined above. For a rigorous mathematical analysis of this model (involving still a certain regularizing term) we refer to [37].

2.1 Mesoscopical description of magnetization

In the classical "microscopical" theory of rigid ferromagnetic bodies as presented by Brown [5] (see also e.g. [4]), based mainly on works of Landau and Lifshitz [21], the conventional description of the state is through the a *"microscopical" magnetization* vector $m = m(x)$ subjected to *Heisenberg-Weiss' constraint*

$$|m(x)| = M_{\rm s} \ , \tag{1}$$

where $M_{\rm s}$ is the *saturation magnetization* at a considered fixed temperature (below Curie's point). In bulks, m typically exhibits fine spatial oscillations, creating a domain structure. In case of soft ferromagnetic materials in the steady state, this can be explained by minimization of the Gibbs's stored energy $G(m) = \int_\Omega \varphi(m(x)) - H(x)\cdot m(x)\,{\rm d}x + \frac12\int_{\mathbb{R}^3}|\nabla u_m(x)|^2\,{\rm d}x$ where $\Omega\subset\mathbb{R}^3$ denotes the domain occupied by the ferromagnet. The first term in G is an *anisotropy energy* with density φ which is an even nonnegative function depending on material properties and exhibiting crystallographic symmetry. The second term in G is an *energy of the interaction* with an applied *external magnetic field* $H = H(x)$ (sometimes called the Zeeman energy). The last term in G is a *magnetostatic energy* involving the scalar potential u_m, induced by the magnetization m and governed by the equation

$$\operatorname{div}(-\mu_0 \nabla u_m + m\chi_\Omega) = 0, \tag{2}$$

where μ_0 is the vacuum permeability and $\chi_\Omega : \mathbb{R}^3 \to \{0,1\}$ is the characteristic function of Ω, i.e. $\chi_\Omega(x) = 1$ if $x \in \Omega$ while $\chi_\Omega(x) = 0$ if $x \notin \Omega$. This form of G is the so-called *no-exchange formulation* which is well acceptable for sufficiently large ferromagnets where an exchange energy contribution is indeed negligible, cf. DeSimone [8]. There is a competition of the anisotropy energy in G preferring the magnetization of the constant length and the demagnetizing field energy preferring it to be zero, which is just what explains quite generic occurrence of the domain microstructure. Mathematically, this is expressed by nonexistence of an exact minimizer of G and by finer and finer self-similar spatial oscillations necessarily developed in any sequence which asymptotically minimizes G.

To pursue evolution in a reasonably efficient manner, it is useful to collect certain information about the fine structure "around" a current point $x \in \Omega$ in the form of a *probability measure*, denoted by ν_x, supported on the sphere $\mathbb{S}^2$ in $\mathbb{R}^3$ of the radius M_s. Hence we write $\nu_x \in \mathrm{M}_0^+(\mathbb{S}^2)$, the set of all probability measures on $\mathbb{S}^2$. Let us furthermore denote the ball $\mathbb{B}^3 = \{M \in \mathbb{R}^3;\ |M| \le M_s\}$ in $\mathbb{R}^3$ of the radius M_s. The collection $\nu = \{\nu_x\}_{x\in\Omega}$ is often called a Young measure [40] and can be considered as a certain "mesoscopical" description of the magnetization. The average, let us call it *macroscopical magnetization*, $M = M(x)$ at a material point $x \in \Omega$ still remains a worthwhile quantity; it is just the first momentum of the Young measure $\nu = \{\nu_x\}_{x\in\Omega}$, i.e.

$$M(x) = \int_{\mathbb{S}^2} m\, \nu_x(\,\mathrm{d}m)\ . \tag{3}$$

Note that the macroscopical magnetization $M : \Omega \to \mathbb{B}^3 \subset \mathbb{R}^3$ "forgets" detailed information about the microstructure in contrast with the mesoscopical magnetization $\nu : \Omega \to \mathrm{M}_0^+(\mathbb{S}^2)$ which can capture *volume fractions* related to particular directions of the magnetization. It should be emphasized that, though we speak about (collections of) probability measures, our approach is *purely deterministic* (not probabilistic).

2.2 Free energy on the mesoscopical level

On the mesoscopical level, we will write the Gibbs' free energy G in terms of the Young measure $\nu = \{\nu_x\}_{x\in\Omega}$ as

$$G(\nu) = \int_\Omega \Big(\int_{\mathbb{S}^2} \varphi(m)\nu_x(\,\mathrm{d}m) \tag{4}$$

$$- H(x)\cdot M(x)\Big)\,\mathrm{d}x + \frac{1}{2}\int\limits_{\mathbb{R}^3} |\nabla u_M(x)|^2\,\mathrm{d}x,$$

where $M = M(\nu)$ according to (3) and u_M is determined by (2) with M instead of m, however. We dare use again the symbol G in (4) because, in fact, this G is merely a continuous extension of the "microscopical" Gibb's energy mentioned in Section 2.1. An interesting property of G is that it is now convex with respect to the natural geometry of the considered parameterized probability measures ν's, let us denote this (also convex) set as $\mathrm{Y}(\Omega;\mathbb{S}^2)$, and that the minimum of G on $\mathrm{Y}(\Omega;\mathbb{S}^2)$ is indeed attained. The mesoscopical steady-state configuration ν minimizing G describes how "to organize" the fine scale structure (microstructure) in order to get the right macroscopic behavior. We refer to [8,13,29,33] for mathematically rigorous reasoning and for a relation between the microscopical and mesoscopical steady-state energy-minimization problems.

2.3 Dissipation potential and rate-independent evolution

Minimization of the free energy (4) can model a steady state or also quasi-stationary evolution under low-frequency applied field $H = H(t)$ of soft magnetic materials with a reasonable accuracy. Varying the applied external magnetic field H then produces only a functional graph on M/H-diagram but no hysteresis loop, where the M/H diagram just means a plot of the spatial average of M vs. H projected into a specific direction. On the other hand, magnetically hard materials exhibit significant hysteresis and thus cannot be modeled by mere minimization of the free energy G. Some approaches to magnetic hysteresis deal with minimization of the "microscopical" free energy (possibly with an exchange-energy term), producing hysteresis due to the nonconvex energy landscape which, however, cannot be controlled by an independent parameter. This cannot reflect, e.g., influence of impurities or dislocations in the atomic grid (which may influence the dissipation without changing considerably the anisotropy energy φ) and may even lead to incorrect numerical effects, cf. [31] where a coercive field for cobalt resulted as 900 Oe instead of an experimentally observed (see [6, p.19]) value 10 Oe.

As the hysteretic response is rate-independent at least for H varying not with too high frequencies, we can be inspired by plasticity theory where so-called Hill's [11] *maximum-dissipation* principle typically governs activated processes arising there. This involves Rayleigh's *dissipation potential* $R = R(\zeta,\dot\nu)$ which is necessarily convex, non-negative and positively homogeneous in terms of rates, i.e. here in terms of $\dot\nu := \mathrm{d}\nu/\,\mathrm{d}t$, and involves also a multiplier ζ to be identified with an activation threshold. This potential R is to describe *phenomenologically* all dissipative mechanisms observed on the mesoscopical

level. This enables us not to have to deal with all details connected with complicated domain evolution on the microscopical level and to model it in a simplified but efficient way only bearing in mind experimentally observed macroscopical energetics. A reasonably general form of R can be, e.g.,

$$R(\zeta,\dot\nu)=\int\limits_\Omega \zeta(x,t)\left|\int\limits_{\mathbb{S}^2}\lambda(m)\dot\nu_x(\,\mathrm{d}m)\right|\mathrm{d}x \tag{5}$$

with $\lambda:\mathbb{S}^2\to\mathbb{R}$ being constant near each pole. Let us confine ourselves to *uni-axial magnets*, which simplifies our considerations (and calculations). Considering the unit vector $e_3=(0,0,1)$ as the easy-magnetization axis, the poles will be at $m=\pm M_{\rm s}e_3$. For dominant anisotropy, one can assume that the magnetization will be mostly in a close vicinity of the poles, i.e. $m\sim\pm M_{\rm s}e_3$, and then the landscape of λ out of the poles is nearly insignificant. Hence one can simply take λ linear:

$$\lambda(m)=m\cdot e_3\equiv m_3\ . \tag{6}$$

In particular, no dissipation (or, equivalently, no activation threshold) appears for changing m_1 or m_2 components of the magnetization vector $m=(m_1,m_2,m_3)$, which agrees with experimental observations for uniaxial ferromagnetical single-crystals. Thus λ basically indicates whether the magnetization lives around the particular pole $m\sim\pm M_{\rm s}e_3$ according to approaching the scalar value $\lambda(m)\sim\pm M_{\rm s}$. As such, λ can be understood as a certain *pole indicator*, playing the rôle of what is often called the "order parameter".

We consider G defined by (4) now with a time-dependent external magnetic field $H=H(x,t)$. We can still formally extend G on the whole space of parameterized measures $L^\infty_{\rm w}(\Omega;M(\mathbb{S}^2))$ by $G(t,\nu)=+\infty$ if $\nu\notin\mathrm{Y}(\Omega;\mathbb{S}^2)$. The desired evolution $\nu=\nu(t)$ is then governed by a simple first-order, doubly nonlinear *differential inclusion*

$$\partial_{\dot\nu}R\Big(\zeta,\frac{\mathrm{d}\nu}{\mathrm{d}t}\Big)+\partial_\nu G(t,\nu)\ni 0 \tag{7}$$

with an initial condition $\nu|_{t=0}=\nu^0$, where the convex set $\partial_\nu G(t,\nu)=\{\omega;\ \forall\tilde\nu:\ G(t,\tilde\nu)\ge G(t,\nu)+\langle\omega,\tilde\nu-\nu\rangle\}$ is the so-called subdifferential of $G(t,\cdot)$. Likewise, the (partial) subdifferential of $R(\zeta,\cdot)$ means $\partial_{\dot\nu}R(\zeta,\dot\nu)=\{\omega;\ \forall\tilde\nu:\ \ R(\zeta,\tilde\nu)\ge R(\zeta,\dot\nu)+\langle\omega,\tilde\nu-\dot\nu\rangle\}$. We refer to [36,37] for more details.

Obviously, (7) can be written as

$$\omega+\partial_\nu G(t,\nu)\ni 0,\quad \omega\in\partial_{\dot\nu}R\Big(\zeta,\frac{\mathrm{d}\nu}{\mathrm{d}t}\Big). \tag{8}$$

By [9, Lemma 4.1(c,d)], the latter inclusion in (8) is equivalent to

$$\Big\langle \frac{\mathrm{d}\nu}{\mathrm{d}t}, \omega \Big\rangle = \max_{\tilde{\omega}\in\mathfrak{C}(\zeta)} \Big\langle \frac{\mathrm{d}\nu}{\mathrm{d}t}, \tilde{\omega} \Big\rangle \tag{9}$$

where the convex set $\mathfrak{C}(\zeta) = \partial_\nu R(\zeta, 0) = \{\omega;\ \forall \nu :\ \langle \omega, \nu\rangle \le R(\zeta, \nu)\}$ determines the region of nondissipative (i.e. nonhysteretic) response. The relation (9) is just what is called the *maximum-dissipation principle*, and expresses the rule that the rate of change of microstructure ν is normal to $\mathfrak{C}$ at ω.

As announced above, the multiplier ζ is, however, not a constant but it is assumed to increase in dependence on the magnetization history at the material point $x \in \Omega$. In view of the special uni-axial case, cf. (6), it seems quite reasonable to consider the activation threshold ζ dependent only on the history of the component M_3 of the macroscopical-magnetization vector $M = M(x,t)$, i.e.,

$$\zeta(x,t) = \max_{0\le\tau\le t} \mathfrak{h}(|M_3(x,\tau)|), \tag{10}$$

where $\mathfrak{h} : [0, M_s] \to \mathbb{R}^+$ is a function describing phenomenologically the activation threshold development process.

Let us mention that we can augment the dissipation potential as well as Gibbs' energy suitably so that one can formulate (7) and (10) in the form of a single doubly nonlinear first-orded inclusion of the type (7) but working with the couple (ν, ζ). This formulation enables, after a certain regularization of Gibbs' energy, a rigorous analysis as far as existence of solutions and their constructive approximation concerns, cf. [37] for details.

2.4 Computer implementation

Though numerical approximation, analysis, and implementation of the model (7) is not the essential point in this paper, we mention only briefly these (otherwise quite important) issues; for more details see [19,37].

We use implicit time discretization of (7) with a constant time step τ. Denoting ν^k the approximate value of $\nu(t)$ at time $t = k\tau$, we consider the so-called backward Euler scheme:

$$\partial_\nu R(\zeta^{k-1}, \frac{\nu^k - \nu^{k-1}}{\tau}) + \partial G(k\tau, \nu^k) \ni 0 \tag{11}$$

for $k = 1, 2, ...$ recursively, with

$$\zeta^{k-1}(x) := \zeta(x,(k-1)\tau) = \max_{0\le l\le k-1} \mathfrak{h}\left(M_3^l\right) \ . \tag{12}$$

When solving (11) for $k=0$, we take ν^0 as the initial condition for (7). Taking into account the convexity of both $R(\zeta^{k-1},\cdot)$ and $G(k\tau,\cdot)$, one can calculate the solution ν^k of (11) simply as a minimizer of the convex function

$$\nu \mapsto G(k\tau,\nu) + \tau R\left(\zeta^{k-1}, \frac{\nu-\nu^{k-1}}{\tau}\right) \tag{13}$$

on the convex set $\mathrm{Y}(\Omega;\mathbb{S}^2)$. For our computational implementation, we used a *finite-element* method (in fact, here rather the finite-volume method) and restricted (13) only on a finite-dimensional convex subset of $\mathrm{Y}(\Omega;\mathbb{S}^2)$ consisting of element-wise constant Young measures. Likewise, ζ^{k-1} from (12) has been restricted in an element-wise constant manner, see [19,36,37] for details.

As the 3-dimensional situation is computationally very demanding, we confine ourselves to axi-symmetric situations that can be reduced to two-dimensional problems. Thus the sphere $\mathbb{S}^2$ reduces to a circle S^1. Moreover, all our examples admit a planar symmetry with respect to the horizontal plane $\{x_3=0\}$, cf. again Figure 1 below, which enables us to make another reduction of variables. The demagnetizing field ∇u_M from (2) produced by a subdomain Ω_j can be calculated for any $x\in\mathbb{R}^3$ exactly through the singular-integral formula

$$\begin{aligned}\nabla u_M(x) = -\frac{1}{\mu_0}\Big(&\int_{\Omega_j} \frac{(x-y)\ \mathrm{div}\, M(y)}{|x-y|^3}\,\mathrm{d}y \\ &- \int_{\partial\Omega_j} \frac{(x-y)M(y)\cdot n(y)}{|x-y|^3}\,\mathrm{d}y\Big),\end{aligned} \tag{14}$$

where n denotes the unit outer normal to the boundary $\partial\Omega_j$ of Ω_j. As we consider the magnetization to be constant within each subdomain Ω_i the first term on the right-hand side of (14) vanishes. Eventually, the second term on the right-hand side of (14) is evaluated using a numerical quadrature rule, which can be considered as a version of the dipole formula; cf. e.g. [31], namely: each subdomain is uniformly copied 18 times by a rotation around x_3 (i.e. each 20 degrees) and magnetization vectors in such a rotated subdomain are considered to be the rotated magnetizations from the original domain.

Although (13) is a nonsmooth problem, it can be turned into a smooth linear-quadratic programming problem with some additional linear constraints and auxiliary variables. The circle S^1 has been discretized to 8 points and the number of elements was 32 on one quarter actually calculated. The resulting

linear-quadratic program was solved by Schittkowski's NLPQL [38]. We refer to [19,36] for implementation details.

3 Computer simulations of CoZrDy ferromagnets

In this section we now want to present usage of the above model for computing the virgin magnetization curve and hysteresis loops of a specific ferromagnetic material. Simulating real experiment, we must naturally set up three mutually independent data sets: material, geometric shape of Ω, and the external magnetic field $H = H(x,t)$.

As to the material, we wanted to choose a uniaxial material with a sufficiently wide parent loop to see clearly minor loops (which excluded Cobalt, e.g.) and with documented material data. To be more specific, let us consider as in [7] a *CoZrDy* homogeneous amorphous alloy (at the temperature 4.2 K) which has indeed a uniaxial structure assumed in (5)–(6) and, moreover, rather small anisotropy to demonstrate efficiency of the method at least in the axisymmetrical case. Let us remark that large anisotropy (e.g. of advanced rare-earth permanent magnets) would cause the magnetization vector to range over only a very small neighborhoods of easy-directions magnetization which would be computationally still much easier. Hence, the *material data* involves in the uniaxial anisotropy energy density in the form

$$\varphi(m) = K \sin^2 \theta \tag{15}$$

with θ the angle between the vectors m and the easy axis (i.e. here $e_3 = (0,0,1)$ in agreement with (6)), the constant $K = 40\ \mathrm{kJ/m^3}$ and the saturation magnetization $M_\mathrm{s} = 0.05\,\mathrm{T}$; cf. [7]. Then, considering the dissipative energy (5)–(6), it remains to determine the function $\mathfrak{h}$ from (12); at this point, however, we have not any specific experiments reported in literature so we have chosen

$$\mathfrak{h}(m_3) = \frac{H_\mathrm{c}}{1.3}\Big(\frac{|m_3|}{M_s} + 0.3\Big) \tag{16}$$

with the *coercive force* $H_\mathrm{c} = 20$ MA/m as in [20]; note that the coercive force is the maximal activation threshold achieved in material magnetized up to saturation. Besides, the choice (16) yields the activation threshold of the demagnetized material as $\mathfrak{h}(0)\doteq 4.6$ MA/m. We always consider a spatially homogeneous time-dependent external magnetic field $H(t) = (0,0,H_3(t))$. Used sawtooth external field $H_3 = H_3(t)$ is shown on Figure 2. In case of Figures 3 and 4, it is not displayed but the reader can easily reconstruct it from the

hysteresis loops because, due to the rate-independence of the model, only its direction and amplitude are of importance.

Finally, the *geometric shape* of a specimen varied. We tested 4 specimens which are axially symmetric with respect to the vertical axis x_3 and symmetric with respect to the horizontal plane $\{x_3 = 0\}$. In all cases, the easy magnetization axis e_3 is vertical, as well as the applied field H, i.e., $H = (0, 0, H_3)$. Cross-sections of the specimens are depicted on Figure 1, including a hypothetical infinitely long specimen (C) which gives an interesting comparison.

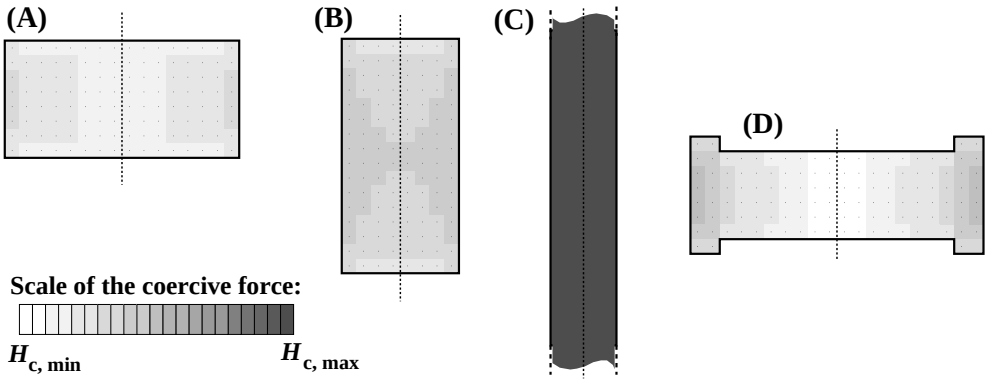

Fig. 1: Cross-sections of the specimens and the distribution of the activation threshold at the first (with respect to process time) local maximum of the external field from Fig. 2.

The resulting hysteretic response is shown on Figure 2. We can see that magnetizing longer magnets produces the hysteresis loops more up-righted in comparison with flat magnets; cf. Fig. 2, the sequence (A)–(B)–(C). The limit case (C) of an infinitely long cylinder magnetized along its easy (=cylindrical) axis makes the demagnetizing field vanish completely, which results in a rectangular hysteresis loop and then the only decisive material data are $\zeta(0)$ and H_c. The fact that an infinitely long cylinder magnetized along its cylindrical (coinciding with the easy) axis produces the zero demagnetizing field is well known and is an example of the so-call *pole avoidance principle*; cf. e.g. [5]. As we infer from (14) the demagnetizing field vanishes if there are no poles, i.e., if $\mathrm{div} M = 0$ in the specimen and M is tangent to the specimen boundary. Note that constant magnetization parallel to the easy axis satisfies this criterion and, moreover, is energetically favorized by φ. Peculiarly, no information about $\mathfrak{h}$, but $\mathfrak{h}(0)$ and $\mathfrak{h}(M_s)$ can be read from this extreme case (C).

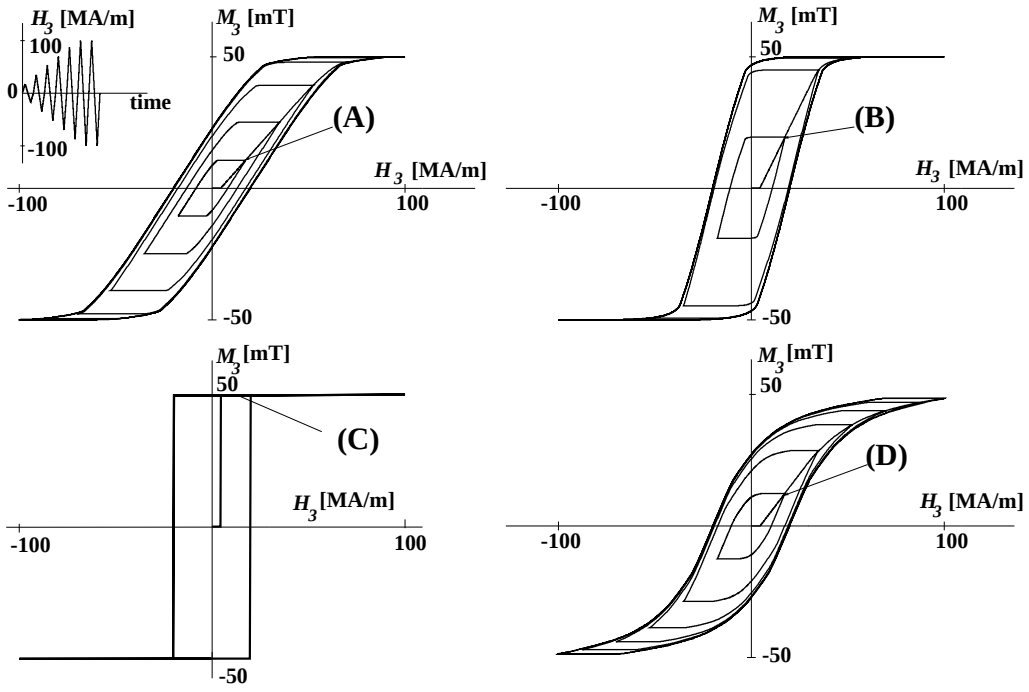

Fig. 2: Virgin magnetization curves and parent loops for the specimens from Fig. 1. The amplitude of external field increases in time according to the left/upper corner diagram; here $K = 40$ kJ/m^3, $M_\mathrm{s} = 50$ mT *and* $H_\mathrm{c} = 20$ MA/m.

The more or less up-righting is a well-known effect usually described, in a very simplified and rough manner, by speaking about a demagnetizing factor. This is indeed rigorous as far as ellipsoidal specimens concerns if magnetized along a main axis. Yet, it is not satisfactory for other shapes especially when they substantially differ from an ellipsoid. This deviation is, in fact, responsible for roundness of hysteretic loops, as shown already in [20]. Our results on Figure 2 (A-B-C) are in agreement with known results (see e.g. [5, Tab. A.3]) saying that the demagnetizing factor of a circular cylinder decreases for "length/diameter" approaching infinity; in particular, Figure 2 (C) shows the impacts of the mentioned pole-avoidance principle on the hysteretic response. Here, Figure 2 (D) shows how even a rather small variation of the shape, cf. Figure 1 (D), can made all hysteretic loops quite substantially more round.

As the activation threshold ζ increases in time differently at particular spots, it is inhomogeneous at particular time instances, and thus we can easily produce minor hysteresis loops as far as the magnetization is not fully saturated in the whole bulk, i.e. if $\zeta \neq H_\mathrm{c}$ at some parts. This is the case of Figure 3.

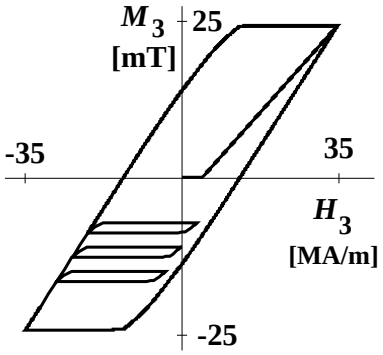

Fig. 3: Minor hysteresis loops due to spatially varying activation threshold resulted by inhomogeneities of magnetization process; case of Specimen (A).

Minor loops are produced by the above model only if the activation threshold ζ is spatially inhomogeneous. After the saturation in a very strong external magnetic fields, the above considered data prevent minor loops. Preservation of minor loops even after the specimen has been saturated can be caused by a material inhomogeneity, e.g., as far as the initial activation threshold $\zeta(0)$ concerns. Let us demonstrate it by considering $\zeta(0) = \zeta(0, x)$ varying randomly with amplitude $\pm 95\%$, i.e. in the interval $[0.23, 9.0]$ MA/m, around the previous value 4.6 MA/m. The resulted minor loops are displayed on Figure 4 for the geometry of Specimen (A) from Figure 1.

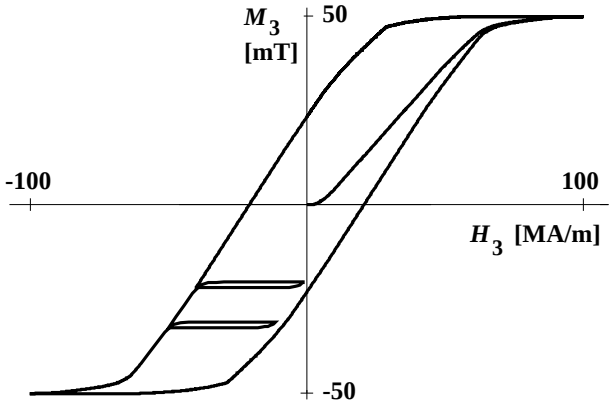

Fig. 4: Minor hysteresis loops in Specimen (A) after saturation due to material inhomogeneities.

4 Conclusions

Using computational modeling, we quantitatively described rate-independent magnetic hysteresis of bulk specimens including the virgin magnetization process and minor loops. This was obtained by counting rigorously mutual interactions of anisotropy and dissipation energies described by an activation

threshold that can possibly increase during magnetization process up to the final threshold, which is what is standardly called the coercive force, and non-local interactions through self-induced demagnetizing field which naturally engages the specimen shape into the calculations. We demonstrated it on simulations of uniaxial CoZrDy ferromagnets which has rather low anisotropy, high-anisotropy advanced rare-earth permanent magnets being computational even easier. Besides explaining one of possible mechanisms leading to rich menagerie of curves inside the parent loops, this method is capable of predicting a hysteresis response of new ferromagnets if the local material properties and the shape of the magnet are known, or of identifying some unknown material properties "cleaned" from influence of the shape of a specimen itself.

References

[1] A. Aharoni, J. Appl. Physics 83 (1998), 3432–3434.

[2] J. Aktaa, A. von der Weth, J. Magnetism & Magn. Mater. 212 (2000), 267–272.

[3] A. Bergqvist, Physica B 233 (1997), 342–347.

[4] G. Bertotti, Hysteresis in magnetism, Academic Press, San Diego, 1998.

[5] W.F. Brown, Jr., Magnetostatic principles in ferromagnetism, North-Holland, Amsterdam, 1962.

[6] S. Chikazumi, Physics of Magnetism. J.Wiley, New York, 1964.

[7] O.A. Chubykalo, J.M. Gonzáles, G.R. Aranda, J. Gonzáles, J. Magnetism & Magn. Mater. 222 (2000), 314–326.

[8] A. DeSimone, Arch. Rat. Mech. Anal. 125 (1993), 99–143.

[9] R.A. Eve, B.D. Reddy, R.T. Rockafellar, Quarterly Appl. Math. 48 (1990), 59–83.

[10] T.L. Gilbert, Phys. Rev. 100 (1955), 1243.

[11] R. Hill, Q.J. Mech. Appl. Math. 1 (1948), 18–28.

[12] A. Hubert, R. Schäfer, Magnetic Domains. Springer, Berlin, 1998.

[13] R.D. James, D. Kinderlehrer, Continuum Mech. Thermodyn. 2 (1990), 215–239.

[14] D. Jiles, Introduction to magnetism and magnetic materials. Chapman & Hall, London, 1991.

[15] D. Jiles, IEEE Trans. Mag. 28 (1992), 2603.

[16] D.C. Jiles, D.L. Atherton, J. Magnetism & Magn. Mater. 61 (1986), 48–60.

[17] M.K. Keane, R.C. Rogers, In: Proc. SPIE (Int. Soc. for Optical Engineering) Vol. 2192, 1994, pp. 52-63.

[18] P.I. Koltermann, at al., Physica B 275 (2000), 233-237.

[19] M. Kružík, Adv. Math. Sci. Appl. (accepted).

[20] M. Kružík, T. Roubíček, J. Magnetism & Magn. Mater., in print.

[21] L.D. Landau, E.M. Lifshitz, Physik Z. Sowjetunion 8 (1935), 153–169.

[22] E.M. Lifschitz, J. Phys. USSR 8 (1944), 337–346.

[23] M. Luskin, L. Ma, SIAM J. Numer. Anal. 29 (1992), 320–331.

[24] L. Ma, Ph.D. Thesis, University of Minnesota, Minneapolis. (1991).

[25] I.D. Mayergoyz, Mathematical Models of Hysteresis. Springer, New York, 1991.

[26] A. Mielke, F. Theil, In: Proc. Models of Cont. Mechanics in Analysis and Engineering, Shaker-Verlag, Aachen, 1999, pp. 117–129.

[27] R.C. O'Handley, Modern Magnetic Materials, J.Wiley, New York, 2000.

[28] J.A. Osborn, Phys. Rev. 67 (1945), 351.

[29] P. Pedregal, Parametrized Measures and Variational Principles, Birkhäuser, Basel, 1997.

[30] F. Preisach, Z. Physik 94 (1935), 277-302.

[31] V. Raposo, J.M. Garcia, J.M. Gonzáles, M. Vázquez, J. Magnetism & Magn. Mater. 222 (2000), 227–232.

[32] Lord Rayleigh, Phil. Mag. 23 (1887), 225–248.

[33] R.C. Rogers, J. Integral Eq. Appl. 3 (1991), 85–127.

[34] T. Roubíček, Relaxation in Optimization Theory and Variational Calculus, W. de Gruyter, Berlin, 1997.

[35] T. Roubíček, In: Comm. Bexbach Coll. on Sci. Vol. II (Eds. M.Robnik, A. Ruffing), Shaker Ver., Aachen,2003, pp. 39–52.

[36] T. Roubíček, M. Kružík, (Preprint No.3/2000, `caesar`, Bonn) Zeit. Angew. Math. Physik, in print.

[37] T. Roubíček, M. Kružík, (Preprint No.27/2002, `caesar`, Bonn,) Zeit. Angew. Math. Physik, accepted.

[38] K. Schittkowski, Annals of Operation Research 5 (1985-6), 485–500.

[39] T. Schrefl, J. Magnetism & Magn. Mater. 207 (1999), 45–65, 66–67.

[40] L.C. Young, Comptes Rendus de la Société et des Lettres de Varsovie, Classe III 30 (1937), 212–234.

[41] A. Visintin, Differential Models of Hysteresis. Springer, Berlin, 1994.

[42] A. Visintin, Physica B 233 (1997), 365–369.

[43] A. Visintin, Physica B 275 (2000), 87–91.

[44] J. Würschmidt, Theorie des Entmagnetisierungsfaktors und der Scherung von Magnetisierungskurven. Vieweg & Sohn, Braunschweig, 1925.